Surface & Coatings Technology xxx (2016) xxx–xxx

Contents lists available at ScienceDirect

Surface & Coatings Technology

journal homepage: www.elsevier.com/locate/surfcoat

Effects of thermal treatment on structure, surface microstructure and optical properties of nitrogen-ion irradiated nanoparticle thin films

Hong-Lian Song, Xiao-Fei Yu, Lian Zhang, Tie-Jun Wang, Mei Qiao, Jing Zhang, Xue-Lin Wang *

School of Physics, State Key Laboratory of Crystal Materials and Key Laboratory of Particle Physics and Particle Irradiation (MOE), Shandong University, Jinan 250100, PR China

ARTICLE INFO

Article history:
Received 14 December 2015
Revised 22 April 2016
Accepted in revised form 4 May 2016
Available online xxxx

Keywords:
Rf-magnetron sputtering
Ion irradiation
X-ray diffraction
Transmittance

ABSTRACT

In this paper, we studied the effects of ion irradiation and annealing treatment on the ZnO thin films. ZnO thin films were first prepared on sapphire substrate by rf-magnetron sputtering technique, followed by nitrogen ion irradiation and annealing treatment. The crystallographic properties, surface morphology and optical properties changed after nitrogen ion irradiation and annealing treatment, which were investigated by X-ray diffraction, scanning electron microscopy and absorption spectroscopy.

1. Introduction

Oxide semiconductor metal nanocomposites, have received great research interest in recent years due to their size-dependent electrical and optical properties, which made these nano-sized materials have potential in energy storage and fluidic sensors [1], optoelectronics [2] and photo catalysis [3]. Because of its wide band gap (3.3 eV), higher transparency in the visible region and large exciton binding energy (60 meV), ZnO is widely used in transparent electronics, UV light emitting devices, invisible field effect transistors and other optical applications [4–6]. The properties of the ZnO nanoparticles depended on the microstructures of the materials, containing crystalline density, crystal size and aspect ratio [7]. Currently, various methods including laser ablation in liquid [3], magnetron sputtering [4–5], thermal evaporation [8], sol-gel technique [9], ion irradiation [2], etc. have been reported for the preparation and modification of ZnO nanostructures. Ion irradiation technique has been widely used for doping in semiconductor yield because it introduces impurity concentrations in selected areas and controlled depths below the surface as well as provides accurate dose control. However, the irradiation process produces undesirable lattice disorder, which can affect the structural and optical electrical properties of the semiconductor. Post irradiation annealing is required to both recover the structure and activate the dopants.

P-type and n-type semiconductor can be obtained from ZnO with different dopants. Group V elements such as N, P and As are used for p-type ZnO [10–11]. Recently, non-metal doped ZnO could effectively improve the light absorption in the visible light activity. Nitrogen has been considered as the potential dopant due to its similarity to oxygen (electronic structure and similar ionic radius), low ionization energy, ease to handle and source abundance [12]. Much experimental work reported about N-doping ZnO films enables the fabrication of transparent conductive devices [13–14]. Many studies on the growth of high quality ZnO thin films have used *c*-plane sapphire as a substrate because of its high crystallinity and low cost [15].

In this work, doped ZnO thin films on sapphire substrate have been achieved by radio-frequency (rf) magnetron sputtering, ion irradiation and annealing treatment at different temperatures. The effect of nitrogen ion irradiation and annealing at different temperatures on the microstructural and optical properties of the doped ZnO nanoparticle thin films were investigated in detail.

2. Materials and methods

Doped ZnO thin films were deposited on seven virgin (0001) oriented sapphire substrates using rf-magnetron sputtering in a mixture of O_2 (content of 6.25%) and Ar (purity, 99.999%). A doped ZnO ceramic target (Er/Yb/ZnO = 1:4:95) with a 3-inch diameter and 0.24-inch thickness was used. The distance between the target and the substrates was 4.7 in. To remove the surface contamination, the substrates were dipped in acetone, rinsed with a large amount of de-ionized water and dried in air before deposition. The substrates were then placed in a chamber where the deposition was performed for 2 h under 4.3×10^{-4} Pa evacuation and an rf power of 120 W at room temperature.

* Corresponding author at: School of Physics, State Key Laboratory of Crystal Materials and Key Laboratory of Particle Physics and Particle Irradiation (MOE), Shandong University, Jinan 250100, PR China.
E-mail address: xuelinwang@sdu.edu.cn (X.-L. Wang).

http://dx.doi.org/10.1016/j.surfcoat.2016.05.014
0257-8972/

Afterwards, samples S11-S61 were irradiated with 90 keV nitrogen ions at a fluence of 1×10^{15} ions/cm^2 at room temperature. The current intensity of the beams is less than 100 μA and the sample temperature of the sample surface below 100 °C during the irradiation. Samples S2-S6 and S21-S61 were thermally annealed at different temperatures as shown in Table 1. A resultant ZnO thin films thickness of 349 nm was achieved which was estimated using the Filmetrics F20. The nitrogen-ion irradiation was simulated using the Stopping and Range of Ions in Matter (SRIM) 2013 software. The structural characterization was performed by X-ray diffraction (XRD) using Cu Kα radiation with a Rigaku RINT-2500VHF. Scanning electron microscopy (SEM) imaging on a Hitachi S-4800 was performed to analyze the sizes and surfaces of the obtained samples. The chemical compositions of the samples were also analyzed with a field emission scanning electron microscope equipped with energy-dispersive spectroscopy (EDS). The absorption spectra of the nanoparticle thin films were measured with an UV–Vis spectrometer with a wavelength range of 200–800 nm.

3. Results and discussion

The simulated atom distribution profile and the stopping power profiles of the incoming nitrogen ions and the schematics of the thin film heterostructure and ion-irradiation are shown in Fig. 1. The density of ZnO and Al_2O_3 are 3.2 g/cm^3, 5.606 g/cm^3, respectively. The displacement thresholds energy of zinc and oxygen are both 57 eV [16], 18 eV for aluminium and 76 eV for oxygen [17]. During the ion irradiation process, the incident nitrogen ions lose energy through elastic collisions (nuclear stopping power) and inelastic collisions (electron stopping power). The nuclear energy loss process dominant in the low energy regime results in a decrease in the physical density [18]. As a result of the collisions between electrons and ions at high ion fluence such as those used in our study, the electronic excitations are known to cause breaking of chemical bonds [19–20]. The range of 90 keV nitrogen ion into the doped ZnO thin films is approximately 576 nm; therefore, the incoming ions are expected to pass through the film (about 349 nm thick), as shown in Fig. 1.

Fig. 2 presents the XRD patterns of 12 samples, which were in good agreement with the standard JCPDS Card of ZnO (No. 36–1451). To reduce the influence of the substrate, we removed the XRD patterns of the Al_2O_3 substrate. The samples exhibit well defined reflection corresponding to (0002) plane of the wurtzite structure of ZnO nanoparticles thin film indicating the films with the *c*-axis normal to the substrate [21]. The full width at half maximum (FWHM) and intensities values of these (0002) peaks changed with different thermal annealing treatment (as shown in Table 2), and the markedly diminished (0002) peaks of these samples indicate deterioration of the nanoparticle film crystallinity and an increase of defects especially after N-ions irradiation. Annealing resulted in the shifting of (0002) diffraction peaks, suggesting the presence of compressive stress in the annealed films.

Table 1
Continuation annealing treatment conditions of the samples in air.

No irradiation	N^+ irradiation	Annealing condition (for 30 min)
S1	S11	At room temperature
S2	S21	100 °C
S3	S31	200 °C
S4	S41	300 °C
S5	S51	400 °C
S6	S61	500 °C

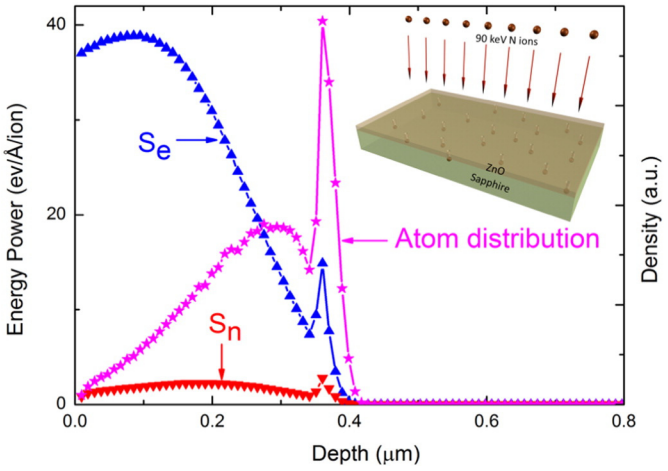

Fig. 1. Electronic, nuclear energy deposition and atom distributions simulated by the SRIM 2013 program. The inset shows the schematic of the thin film heterostructure and normal incidence of ions.

The lattice constant *a* and *c* of the wurtzite structure have been determined by the following formula [22]:

$$d_{hkl}^2 = \left(\frac{4\left(h^2 + hk + k^2\right)}{3a^2} + \frac{l^2}{c^2} \right)^{-1} \quad (1)$$

where d is the interplanar space and h, k, l are miller indices. For (0002) peak h, k, l are 0, 0, and 2 respectively. The calculated lattice constant c is given in Table 2. It clearly shows that c values decreased after *N*-ion irradiation and increasing annealing temperature.

To obtain detailed structural information, the average crystallite size was calculated from the FWHM of the (0002) diffraction peak according to the Debye-Scherer equation [23]:

$$D = \frac{K\lambda}{\beta \cos \Theta} \quad (2)$$

where *D* is the crystallite size, *k* is a constant of 0.89, λ is the X-ray wavelength (0.15406 nm), β is FWHM, and Θ is the Bragg angle of the (0002) peak. The variations are shown in Table 2.

As we can see from Fig. 2, after nitrogen ion irradiation, the (0002) peak shifted to the large angle range, which demonstrated that nitrogen

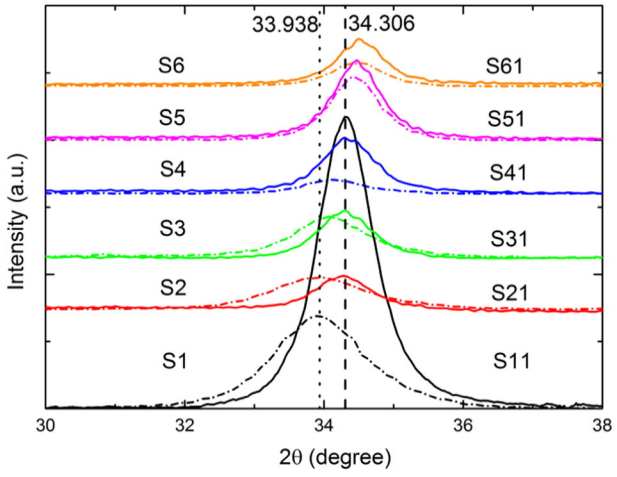

Fig. 2. XRD pattern of the obtained films showing the (0002) ZnO peaks. Short dash dot line are the samples S1-S6, straight line are samples S11-S61, the dot line is the 2Θ for S1 and the short dash line is the 2Θ for S11.

Please cite this article as: H.-L. Song, et al., Surf. Coat. Technol. (2016), http://dx.doi.org/10.1016/j.surfcoat.2016.05.014